View metadata, citation and similar papers at core.ac.uk
brought to you by CORE
provided by Archivio istituzionale della ricerca - Università dell'Insubria

Volume Reflection Dependence of 400 GeV/c Protons on the Bent Crystal Curvature

W. Scandale,[1] A. Vomiero,[2] S. Baricordi,[3] P. Dalpiaz,[3] M. Fiorini,[3] V. Guidi,[3] A. Mazzolari,[3] R. Milan,[4] Gianantonio Della Mea,[5] G. Ambrosi,[7] B. Bertucci,[6,7] W. J. Burger,[6,7] M. Duranti,[6,7] P. Zuccon,[7] G. Cavoto,[9] F. Iacoangeli,[8] C. Luci,[8,9] S. Pisano,[8] R. Santacesaria,[9] P. Valente,[9] E. Vallazza,[10] A. G. Afonin,[11] Yu. A. Chesnokov,[11] V. I. Kotov,[11] V. A. Maisheev,[11] I. A. Yazynin,[11] A. D. Kovalenko,[12] A. M. Taratin,[12] A. S. Denisov,[13] Yu. A. Gavrikov,[13] Yu. M. Ivanov,[13] L. P. Lapina,[13] L. G. Malyarenko,[13] V. V. Skorobogatov,[13] V. M. Suvorov,[13] S. A. Vavilov,[13] D. Bolognini,[14] S. Hasan,[14] D. Lietti,[14] A. Mozzanica,[14] and M. Prest[14]

[1]*CERN, European Organization for Nuclear Research, CH-1211 Geneva 23, Switzerland*
[2]*INFM-CNR, Via Vallotti 9, 25133 Brescia, Italy*
[3]*INFN Sezione di Ferrara, Dipartimento di Fisica, Università di Ferrara Via Saragat 1, 44100 Ferrara, Italy*
[4]*INFN Laboratori Nazionali di Legnaro, Viale Università 2, 35020 Legnaro (PD), Italy*
[5]*Dipartimento di Ingegneria dei Materiali e Tecnologie Industriali, Università di Trento, Via Mesiano 77, 38050 Trento, Italy*
[6]*Dipartimento di Fisica, Università degli Studi di Perugia via Pascoli, 06123 Perugia, Italy*
[7]*INFN Sezione di Perugia, via Pascoli, 06123 Perugia, Italy*
[8]*Dipartimento di Fisica, Università di Roma 'La Sapienza' Piazzale A. Moro 2 I-00185 Rome, Italy*
[9]*INFN Sezione di Roma, Piazzale Aldo Moro 2, 00185 Rome, Italy*
[10]*INFN Sezione di Trieste, Via Valerio 2, 34127 Trieste, Italy*
[11]*Institute of High Energy Physics, Moscow Region, RU-142284 Protvino, Russia*
[12]*Joint Institute for Nuclear Research, Joliot-Curie 6, 141980, Dubna, Moscow Region, Russia*
[13]*Petersburg Nuclear Physics Institute, 188300 Gatchina, Leningrad Region, Russia*
[14]*Università dell'Insubria, via Valleggio 11, 22100 Como, Italy & INFN Sezione di Milano Bicocca, Piazza della Scienza 3, 20126 Milano, Italy*

(Received 22 October 2007; published 1 December 2008)

The trend of volume reflection parameters (deflection angle and efficiency) in a bent (110) silicon crystal has been investigated as a function of the crystal curvature with 400 GeV/c protons on the H8 beam line at the CERN Super Proton Synchrotron. This Letter describes the analysis performed at six different curvatures showing that the optimal radius for volume reflection is approximately 10 times greater than the critical radius for channeling. A strong scattering of the beam by the planar potential is also observed for a bend radius close to the critical one.

DOI: 10.1103/PhysRevLett.101.234801 PACS numbers: 29.27.−a, 42.79.Ag, 61.85.+p

When high-energy charged particles enter a crystal with a small incidence angle with respect to the crystal planes (θ_0), their motion in the transverse direction is determined by $U(x)$, the crystal potential averaged along the planes. If $|\theta_0|$ is smaller than a critical value $\theta_c = (2U_0/pv)^{1/2}$ (where p and v are the particle momentum and velocity and U_0 is the planar potential well depth), the particle can be captured in the channeling regime, oscillating between two neighboring planes. The angular acceptance for channeling is thus of $\pm\theta_c$. θ_c is about 10 μrad for 400 GeV/c protons in a (110) silicon crystal.

Even when the crystal is bent, particles can be channeled (and thus deflected) if the bend radius R is greater than a critical value $R_c = pv/eE_m$ [1], where E_m is the maximum strength of the electric field in the channel. For a (110) silicon crystal, $E_m \approx 6$ GV/cm and for 400 GeV/c protons $R_c = 68$ cm.

The transverse motion of a channeled particle in a bent crystal is governed by the effective potential [2] $U_{ef}(x, F_c) = U(x) + F_c x$, where $F_c = pv/R$ is the centrifugal force and the x coordinate is measured in the direction opposite to the radial one (Fig. 1). The centrifugal term leads to the inclination of the effective potential and to the reduction of the outer wall in each channel. This effect, in turn, decreases the critical channeling angle, the capture probability P_c of particles into the channeling regime and the dechanneling length L_d [2–4]. The potential well fully disappears and the channeling regime is no longer possible, when the bend radius R is equal or smaller than R_c.

In a bend crystal with $R > R_c$, if $|\theta_0| > \theta_c$, the particle is not captured into the channeling regime at the crystal entrance. However, if the particle momentum has a tangency point with the bent planes within the crystal volume, the effect of volume reflection (VR) can take place [5,6]. Because of this effect almost all particles are deflected to the opposite direction with respect to the crystal bending. A beam deflection with efficiency greater than 95% due to VR has been experimentally observed at the CERN SPS with 400 GeV/c protons [7]. Moreover, VR can deflect particles in a range of θ_0 much wider than for channeling. This range is equal to the crystal bend angle.

This Letter presents the measurements of the VR parameters—the mean deflection angle θ_{vr}, its rms deviation σ_{vr} and the efficiency P_{vr}—as a function of the bend

 © 2008 The American Physical Society

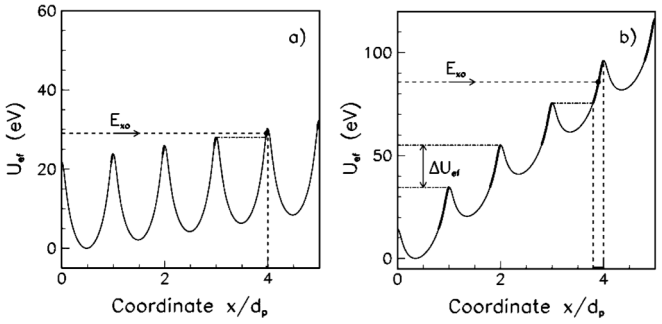

FIG. 1. The effective potentials for the (110) planes of a silicon crystal bent with a radius $R = 35.71$ m (a) and 3.76 m (b) for 400 GeV/c protons. The coordinate x is measured in the direction opposite to the radial one; $d_p = 1.92$ Å is the planar channel width (distance between the two walls of each potential well) and $\Delta U_{ef} = (pv/R)d_p$ is the potential inclination along the channel. The trajectory of a particle being reflected with a turning point in the fourth channel is shown. The position of the corresponding reflecting plane is shown by a vertical dashed line at $x = 4d_p$. The thicker lines show the turning point regions.

radius R of a (110) silicon strip crystal. Results are compared with Monte Carlo (MC) simulation and analytical calculations.

As experimentally observed, if $\theta_0 > \theta_c$, most of the incident particles are deflected because of VR to a direction opposite to the crystal bending by an angle of about $1.5\theta_c$. A small part of them, on the contrary, is captured into the channeling regime along the tangency area (volume capture, VC), once their transverse momentum has been reduced by multiple scattering with the crystal nuclei and electrons [8,9]. The VC probability dependence on the crystal radius R is approximately linear ($P_{vc}(R) \approx R\theta_c/L_d$ [10,11]) due to a linear increase of the tangency region length with increasing R. Since VC limits the VR efficiency, that is $P_{vr}(R) = 1 - P_{vc}(R)$, the VC dependence on R translates in a linear decrease of the VR efficiency with increasing R.

It is shown in [5,6] that in a bent crystal the distribution of the particle deflection angles due to VR is broadened if the centrifugal force F_c acting on the particles increases, which means that for particles of a given energy E a larger crystal curvature leads to a smaller θ_{vr} and a larger σ_{vr}. Such a change of the VR parameters becomes clear when the effective potential variation as a function of the crystal curvature is considered (Fig. 1). VR occurs near the turning points of quasichanneled particles in the effective potential of a bent crystal, where the particles radial velocity changes its sign.

For a small crystal curvature, that is $R \gg R_c$, the turning points of all particles gather in a narrow region near the inner wall of a planar channel [Fig. 1(a)]. The strong electric field of the crystal plane is directed along R and at the turning points it imparts to the particle an angular deflection towards the opposite direction with respect to the crystal bending, producing volume reflection. For larger crystal curvatures, the turning region of the effective potential increases. This decreases the electric field value at the lower boundary of the turning region and therefore, the average deflection angle due to VR becomes smaller. At the same time, the range of field values near the turning points gets larger and this increases the spread of the particles deflection angles.

For crystal bend radii $R \leq R_c$, the channel potential well disappears and the radial momentum turning of particles in the effective potential can occur anywhere across the channel. For particles whose turning points are located near the channel outer wall, the electric field of the plane, which is directed opposite to R, gives an angular deflection towards the bending side. Therefore, the particle deflection angle averaged over the turning point positions in the effective potential across a whole channel becomes close to zero.

The experimental setup to collect the data presented in this Letter consisted of four double-sided microstrip silicon detectors [SiX in Fig. 2(a)] for single track reconstruction with an intrinsic angular resolution of 0.4 μrad, which is

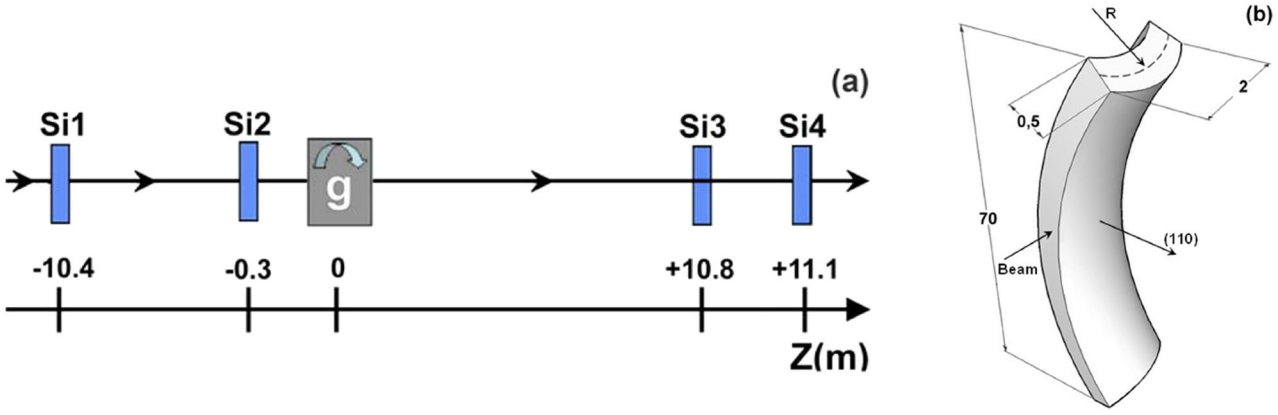

FIG. 2 (color online). (a) Experimental layout on the H8 beam line at the CERN SPS. Si1-Si4 are the silicon microstrip detectors, g is the goniometer. (b) View of the (110) silicon crystal strip bent along its height (principal bending). The anticlastic bending with a radius R generated along the strip width has been used for the beam deflection. The beam axis line is shown and the dimensions of the crystal given in mm.

TABLE I. VR parameters for the different crystal bend radii R.

$R(m)$	θ_{vr} (μrad)	$\bar{\sigma}_{vr}$ (μrad)	ε (%)
2.41	$5.43 \pm 0.10 \pm 0.64$	$6.39 \pm 0.08 \pm 0.47$	$1.56 \pm 0.11 \pm 0.1$
3.76	$8.68 \pm 0.14 \pm 1.19$	$4.50 \pm 0.12 \pm 0.42$	$2.07 \pm 0.21 \pm 0.8$
4.49	$9.89 \pm 0.09 \pm 0.68$	$3.80 \pm 0.08 \pm 0.33$	$2.64 \pm 0.16 \pm 0.4$
8.7	$12.48 \pm 0.08 \pm 0.45$	$1.76 \pm 0.07 \pm 0.17$	$3.98 \pm 0.19 \pm 0.2$
20.85	$13.90 \pm 0.16 \pm 0.49$	$1.68 \pm 0.15 \pm 0.22$	$5.52 \pm 0.31 \pm 0.9$
35.71	$14.08 \pm 0.11 \pm 0.41$	$1.10 \pm 0.11 \pm 0.09$	$6.22 \pm 0.38 \pm 1.5$

negligible with respect to the total resolution (about 3 μrad) due mainly to multiple scattering in the detector material and in the air. A $70 \times 2 \times 0.5$ mm^3 silicon crystal strip obtained from a wafer by means of anisotropic chemical etching [12] was used. Its largest faces are parallel to the (110) crystallographic planes and it was bent along its length [Fig. 2(b)]. The anticlastic curvature acquired along the crystal width was used for the beam deflection as it was first suggested in [13] and was changed by changing the principal bend radius of the crystal itself.

The particle deflection angle was computed as $\theta_{\text{out}} - \theta_{\text{in}}$ where θ_{in} is the incoming angle of a particle to the crystal (reconstructed with Si1 and Si2) and θ_{out} is the outgoing angle, measured with Si2 and either Si3 or Si4. To select only particles hitting the crystal and to reduce background events, requirements on the horizontal and vertical positions of the particle impact point on the crystal were imposed.

The crystal was positioned on a high precision goniometer (g in Fig. 2(a)] that allowed to align it with respect to the beam. When the crystallographic planes are far from the beam axis direction, particles experience the usual multiple Coulomb scattering in the crystal. In this case, the deflection angle distribution has a Gaussian shape with mean θ_{am} and rms deviation σ_{am} which has been measured to be (5.59 ± 0.11) μrad. For specific crystal orientations, the beam is deflected due to either channeling or VR with mean values θ_{ch} and θ_{vr}, respectively.

The crystal has been aligned at the maximal channeling position and, in the assumption of a uniform bending, the crystal bend radius R has been obtained from the channeling deflection angle θ_{ch} as $R = L/\theta_{ch}$ where L is the crystal length along the beam direction (2 mm). The values for R obtained in this way are listed in Table I. The smallest bend radius, $R = 2.41$ m, is about 3 times greater than R_c.

The definitions of the VR main parameters are illustrated in Fig. 3, where the angular distributions of protons for two bend radii (8.7 m and 36.62 m) are shown. A Gaussian fit to the deflection angle distributions gives the mean θ_{vr} and its rms deviation σ_{vr}. The value of $\theta_{vr} + 3\sigma_{vr}$ determines the boundary between the volume-reflected portion of the beam and the nonreflected beam, which is due to the volume capture of protons, and allows to compute the VR inefficiency ε. Finally, $\bar{\sigma}_{vr} = \sqrt{\sigma_{vr}^2 - \sigma_{am}^2}$ describes the angular spread due to the potential scattering of protons in the crystal.

The results are shown in Table I. The systematic errors have been estimated changing the cuts both in angles and positions of the particles on the crystal. The resulting variation in the parameters values could be caused by the presence of some nonuniformity of the crystal anticlastic bending.

Figure 4 shows the experimental dependencies of θ_{vr} and σ_{vr} on the crystal curvature and the dependence of ε on the crystal bend radius R. In the measured range the mean deflection angle θ_{vr} decreases approximately linearly as the curvature increases. This is similar to the dependence of the critical channeling angle in case of moderate crystal bending [2,3] ($\theta_c(R) \sim 1 - R_c/R$). As in the case of θ_c whose decrease is caused by the decrease of the potential well depth, the decrease of θ_{vr} occurs because the effective potential tends to a straight line.

On the contrary, the rms deviation σ_{vr} increases approximately linearly within the measured range of crystal curvatures. This increase is caused by the increase in the spread of the electric field strength near the turning points in the effective potential. The results of a simulation based on the model of planar channeling in a bent crystal (PCinBC) developed in [9] and the results obtained by using the explicit expression for the VR deflection angle [14] are both shown in Fig. 4. The silicon atom potential obtained through the experimental x-ray scattering factors was used in both cases. According to this model, σ_{vr}

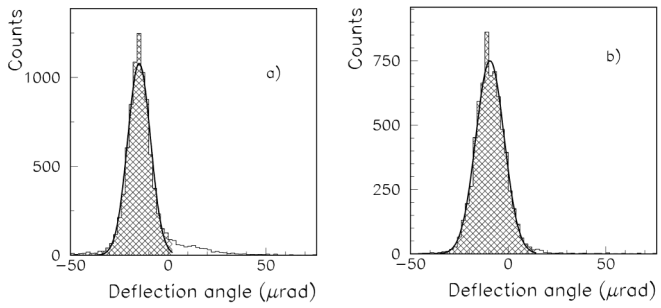

FIG. 3. The deflection angle distribution of the 400 GeV/c proton beam due to VR in the (110) silicon crystal bent with $R = 35.71$ m (a) and $R = 3.76$ m (b). The parameters of the Gaussian fit: the mean deflection angle $\theta_{vr} = 14.08$ μrad (a) and 8.68 μrad (b); the rms deviation $\sigma_{vr} = 5.70$ μrad (a) and 7.28 μrad (b). The hatched histogram area with angles smaller than $\theta_{vr} + 3\sigma_{vr}$ defines the VR efficiency P_{vr}.

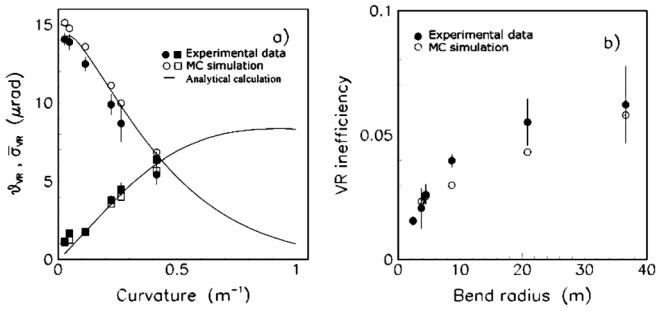

FIG. 4. The dependencies of the VR parameters on the crystal curvature and the bending radius R: (a) the deflection angle θ_{vr} (dots) and its rms deviation due to the potential scattering $\bar{\sigma}_{vr}$ (squares), (b) the VR inefficiency ε.

achieves its maximum value at a bend radius of about 1.1 m (approximately $1.6R_c$), and decreases with decreasing R because the effective potential becomes closer to a straight line. The reflection inefficiency ε increases with R since the VC probability increases. The simulation results show an almost linear dependence as expected by the theoretical estimation for the VC probability.

The agreement between the experimental data, the analytical approach and the MC simulation is fairly good. The discrepancy could be the result of a nonuniformity of the anticlastic bending so that the real curvature in the middle of the crystal is greater than the average one.

Taking into account the observed dependences of the VR parameters on R, an optimal bend radius for a short silicon crystal for beam deflection due to VR is found to be about $10R_c$. This value maximizes the product of the deflection angle times the reflection efficiency times the angular acceptance. The increase of R gives larger θ_{vr} but decreases the efficiency and the angular acceptance. To obtain the same acceptance, the crystal length should be increased but this generates more particle losses in inelastic interactions with the crystal nuclei.

A strong potential scattering of particles for R close to R_c shows that such a crystal can be used as an effective scatterer. The thickness of the crystal scatterer can be reduced down to the wavelength of the particle oscillations in the planar channel (60 μm for 400 GeV protons and 250 μm for 7 TeV protons). In this way the inelastic losses of particles in the scatterer can be minimized.

The experimental studies performed by the H8RD22 collaboration show that a short bent crystal (or a sequence of them) in the VR operational mode can be used as a primary collimator for modern hadron colliders where the collimation system is fundamental to protect the accelerator components from radiation damage and to reduce the experiments background. Such a crystal collimator can deflect the beam halo particles directing them into a secondary collimator whereas a standard amorphous primary collimator scatters particles in both sides around the initial direction. A crystal primary collimator would increase the efficiency of the collimation system, reducing impedance and the requirements on the alignment of the secondary collimator.

We are grateful to Professor L. Lanceri (INFN & University of Trieste) who provided the tracking detectors. We acknowledge partial support by the European Community-Research Infrastructure Activity under the FP6 ''Structuring the European Research Area'' program (CARE, contract number RII3-CT-2003-506395), the INFN NTA-HCCC, the INTAS program and MIUR 2006028442 project, Russian Foundation for Basic Research Grants 05-02-17622 and 06-02-16912, RF President Foundation Grant SS-3057-2006-2, Program ''Fundamental Physics Program of Russian Academy of Sciences.''

[1] E. Tsyganov, Preprint TM-682, TM-684, Fermilab, Batavia (1976).
[2] V. V. Kaplin and S. A. Vorobiev, Phys. Lett. A **67**, 135 (1978).
[3] A. M. Taratin and S. A. Vorobiev, Phys. Status Solidi B **107**, 521 (1981).
[4] J. A. Ellison and S. T. Picraux, Phys. Lett. A **83**, 271 (1981).
[5] A. M. Taratin and S. A. Vorobiev, Nucl. Instrum. Methods Phys. Res., Sect. B **26**, 512 (1987).
[6] Y. M. Ivanov *et al.*, Phys. Rev. Lett. **97**, 144801 (2006).
[7] W. Scandale *et al.*, Phys. Rev. Lett. **98**, 154801 (2007).
[8] V. A. Andreev *et al.*, JETP Lett. **36**, 415 (1982).
[9] A. M. Taratin and S. A. Vorobiev, Sov. Phys. Tech. Phys. **30**, 927 (1985).
[10] Yu. A. Chesnokov *et al.*, Nucl. Instrum. Methods Phys. Res., Sect. B **69**, 247 (1992).
[11] V. Biryukov, Phys. Lett. A **205**, 340 (1995).
[12] S. Baricordi *et al.*, Appl. Phys. Lett. **91**, 061908 (2007).
[13] A. G. Afonin *et al.*, Phys. Rev. Lett. **87**, 094802 (2001).
[14] V. A. Maisheev, Phys. Rev. ST Accel. Beams **10**, 084701 (2007).